Draft version September 18, 2016
Preprint typeset using LaTeX style emulateapj v. 12/16/11

SPECIFIC FREQUENCY FOR 20 NUCLEATED DWARF ELLIPTICALS IN VIRGO CLUSTER

Lingjian Chen
Department of Physics and Astronomy, Shanghai Jiao Tong University, Shanghai 200240, China
Draft version September 18, 2016

ABSTRACT

Globular culsters (GC) are the tracers of galaxy evolution, richness and other properties of GC systems can help make clear formation history and constrain models. Thanks to the deep image from Next Generation Virgo Cluster Survey (NGVS), we have calculated specific frequency ($S_{\rm N}$) for 20 nucleated dwarf ellipticals in Virgo cluster, all of which are fainter than $M_V = -16.5$, and found that their $S_{\rm N}$ is significantly larger and scattered than massive galaxies and the trend shows $S_{\rm N}$ increases monotonically with M_V at $M_V > -16.5$. We also studied GC colr distribution and the influence of environment on GC richness of galaxies. Our work suggests the ... model may be a good explanation of evolution of dE,Ns.

Subject headings: globular clusters, specific frequency, dwarf ellipticals

1. INTRODUCTION

The idea of specific frequency was proposed by Harris and van den Bergh (1981) in order to investigate the richness of GCs for individual galaxies nomalized to host galaxy luminosity in V band. Conventionally, it is written as:

$$S_{\rm N} = N_{\rm GC} \times 10^{(M_V+15)} \tag{1}$$

where N_{GC} the number of GCs a galaxy owns. Peng et al. (2008) used M_z and calculate $S_{N,z}$ instead of M_V in that M_z traces stellar mass better.

Another indicator of richness of GCs was proposed by Zepf and Ashman (1993) and is written as:

$$T = \frac{N_{\rm GC} \times M_*}{10^9 M_\odot} \tag{2}$$

T is normalized to host galaxy mass (M_* is the stellar mass of the galaxy), instead of luminosity, so comparison of T among different types of galaxies are more physically intrinsic than comparison of $S_{\rm N}$, however, in the meantime, it is more difficult to get in optical bands (easier and more accurate in infrared).

Study of specific frequency can constrain some models of galaxy evolution, especially their star formation history and GC formation efficiency. Recent studies (e.g Brodie and Strader (2006), Peng et al. (2008), Georgiev et al. (2010) and Harris et al. (2013)) have shown that $S_{\rm N}$ is quite low and cosntant for midsized galaxies, but shows uprise at both high-mass and low-mass end, generally showing a U shape.

It is very appealing to study the low-luminosity and of the $S_{\rm N} \sim M_V$ relationship epecially through nucleated dwarf ellipticals (dE,Ns) as the mechanism of their evolution is not quite clear yet and study of them may reveal new interpretations of $S_{\rm N}$ relationship with other galactical arameters. The question lingers that whether dE,Ns are intrinsically more efficient in making GCs or their field stars are largely stripped and thus make them relatively GC-rich.

Another puzzuling problem is the $S_{\rm N}$ dependence on the environment, as it seems that galaxies near the center of galaxy clusters are more likely to have high $S_{\rm N}$ than those who are far away from cluster center or not in a cluster.[*citation needed*]

fiorano_chen@sjtu.edu.cn

In this paper, we focoused on the low-luminosity galaxies and implemented eq.1 to measure the richness of GC systems in 20 dE.Ns (assuming they have the same M/L ratio). In §2, we will show the data collection and how we count the GCs, the findings for $S_{\rm N}$ (luminosity and environmental dependence, and GC color distribution) are listed in §3. Discussions for the findings are listed in §4 and conclusions in §5.

2. DATA RETRIVEMENT AND PROCESSING

2.1. *Data Reducion*

The Next Generation Virgo cluster Survey (NGVS) provides a wide-range but also deep and homogeneous catalog within the Virgo cluster (Ferrarese et al. (2012)), which allows us to detect the GCs around very faint dE.Ns. The data reduction and photometry pipeline follows the general process in NGVS, for detail see Ferrarese et al. (2012) and Liu et al. (2015). When detecting objects in NGVS fields, the galaxy light is not subtracted, thus leaving some GCs near galaxy center undetected, which reduced our detection efficiency and may lower our GC counts. Our original sample contains 704 spectroscopically confirmed Virgo Cluster members, then 20 dE,Ns are selected from them through visual inspection, summary of their data is given in table.1; nine samples of our candidates are pictured in fig.1.

The essential parameters for calculating $S_{\rm N}$ are number of GCs ($N_{\rm GC}$) and absolute magnitude in V band. To find $N_{\rm GC}$, we need to choose the area in which we count them, which has to do with effective radius. For M_V, we need to find out the apparent magnitude and distance.

Effective radii (R_e) of each galaxy are retrieved from SDSS DR6's half flux radius `petro_R50`. And the radius for counting the GC systems is set at $R_c = 4R_e$, we adjust R_c to this value mainly for the comparison with the literature and minimize the error (with no particular physical reasons), the GCs detected within this radius are counted as members of the galaxy's GC system.

TABLE 1
PHOTOMETRIC AND DERIVED PROPERTIES OF 20 DE,NS

Index (1)	other name	RA	DEC	u (2)	g (2)	z (2)	r_e (3)	r_p (4)(Mpc)	DM (5)	M_V	S_N	M_z (6)	$S_{N,z}$
0032	VCC0235	184.36064	13.73703	19.42	17.24	16.37	11.07	1.04	31.9	-15.1	20.1±3.6	-15.6	12.7±2.3
0042	IC3142	184.75826	13.98245	17.91	15.92	14.73	12.82	0.96	31.0	-15.7	12.6±1.0	-16.3	7.2±0.6
0044	VCC0330	184.80190	12.85187	18.30	16.94	15.98	9.09	0.85	31.0	-14.6	11.6±11.6	-15.1	7.3±7.3
0059	VCC0426	185.15133	12.88475	19.68	18.10	17.18	8.41	0.75	31.6	-14.0	30.1±0.0	-14.5	19.0±0.0
0096	VCC0695	186.02193	10.06775	18.73	16.31	15.41	10.94	0.83	31.7	-15.8	6.7±1.9	-16.3	4.2±1.2
0119	VCC0812	186.39515	15.19439	18.60	16.92	15.97	8.92	0.89	32.0	-15.6	9.2±0.0	-16.1	5.8±0.0
0125	VCC0833	186.43600	13.02210	18.46	16.88	15.73	7.40	0.41	30.8	-14.4	13.9±3.5	-15.1	7.3±1.8
0131	VCC0872	186.52787	12.86098	18.13	16.67	15.54	7.37	0.37	31.8	-15.6	4.6±4.6	-16.3	2.4±2.4
0146	VCC0931	186.68337	10.90480	18.16	16.57	15.77	10.77	0.52	30.4	-14.3	57.2±3.8	-14.7	39.5±2.6
0164	VCC1005	186.85599	13.75081	17.77	16.36	15.23	9.98	0.46	32.9	-17.1	1.7±0.6	-17.7	1.0±0.3
0180	VCC1079	187.05011	10.36533	18.54	16.94	16.08	11.64	0.61	32.0	-15.6	13.8±3.5	-16.0	9.6±2.4
0181	VCC1076	187.05345	10.52604	18.99	17.54	16.79	10.17	0.57	32.4	-15.3	9.1±0.0	-15.6	6.9±0.0
0184	VCC1093	187.07809	11.70029	17.91	16.35	15.30	9.99	0.27	32.0	-16.0	6.4±0.8	-16.7	3.3±0.4
0187	VCC1107	187.12701	7.32475	17.76	16.11	14.93	10.95	1.47	32.0	-16.4	8.3±3.3	-17.1	4.3±1.7
0194	NGC4472DW05	187.17306	7.80424	18.37	17.12	16.22	8.09	1.33	31.1	-14.4	7.0±0.0	-14.9	4.4±0.0
0254	VCC1218	187.43842	5.92023	18.27	16.28	15.42	11.75	1.87	31.1	-15.3	7.6±3.0	-15.7	5.2±2.1
0313	VCC1264	187.54536	12.19550	18.49	17.17	16.43	9.35	0.07	31.0	-14.3	38.1±3.8	-14.6	28.9±2.9
0443	NGC4472DW04	187.75470	7.72322	19.26	17.40	16.53	9.37	1.34	31.7	-14.7	18.5±5.3	-15.2	11.6±3.3
0573	SDSS object[a]	188.29234	12.08609	20.87	20.23	18.97	2.65	0.19	31.0	-11.2	0.0±0.0	-12.1	0.0±0.0
0686	VCC2014	191.29036	10.63038	19.33	18.13	17.00	10.44	1.15	31.2	-13.5	31.8±15.9	-14.2	16.7±8.4

[1] This Index is given among original 704 candidates
[2] appranent magnitude from SDSS DR6
[3] r_e = effective radius = half-petrosian flux radius in arcsec, from SDSS DR6
[4] r_p is defined as the projected distance form the Virgo Cluster center, M87
[5] DM=distance modulus, from NED
[6] This is calculated from $z_{\rm SDSS}$
[a]SDSS J123310.16+120509.9

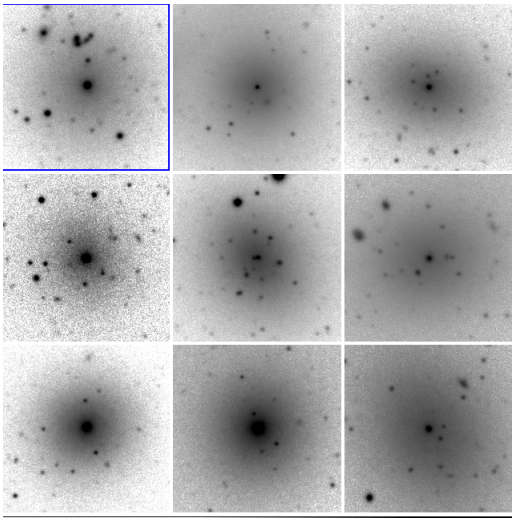

FIG. 1.— Nine candidates of dE.Ns. From left to right and top to bottom: 0032, 0042, 0044, 0059, 0096, 0119, 0125, 0131, 0146. Each of them clearly shows a nuleus.

Magnitude data (u, g, z bands) are also taken from SDSS DR6. After retriveing the data, we convert magnitudes in SDSS system into UBV system[1]:

$$V = g - 0.59(g - r) - 0.01 \quad (3)$$

Distance modulus (DM) needed for converting apparent magnitude V to absolute magnitude M_V are taken from NED (we use DM calculated from luminosity distance). For those galaxies which don't have DM data on NED, we use DM = 31.0($\sim$ 16.5Mpc) as it is the average DM for objects in Virgo cluster.

[1] http://classic.sdss.org/dr4/algorithms/sdssUBVRITransform.html

2.2. *GC selection*

GCs are selected through color-color diagrams among all detected objects in the NGVS(for example, see fig.3). The selection criteria is taken from Liu et al. (2015) and is adjusted according to spectroscopic data by Hubble Space Telescope (HST) ACSVCS project on VCC1545(see fig.2) to reach the maximum match.

$$18.5 < g < 24.4 \quad (4a)$$
$$0.8 < u - g < 1.79 \quad (4b)$$
$$0.62 < g - z < 1.5 \quad (4c)$$
$$0.95(u - g) - 0.31 < g - z < 0.77(u - g) + 0.35 \quad (4d)$$
$$-0.15 < i_4 - i_8 < 0.25 \quad (4e)$$

Eq.4b through eq.4d enclose a polygon area on the color-color diagram, and eq.4e is the constriant on the diffusiveness of the object.

We estimate the error of $S_{\rm N}$ by cutting a annulus around the counting area, which has the same area with the counting area (circle with radius R_c), and then we count every GC we find in this annulus as a contamination object. This error of GC counting is then propagated into error of $S_{\rm N}$.

Finally, we double both the GC counts and contaminations to correct for the real number because the GC luminosity function (GCLF) is assumed to be gaussian and peak at around $M_V = -7.4$ ($m_V = 24.4$ for DM=31.0 of Virgo cluster, close to our choice of truncation mag-

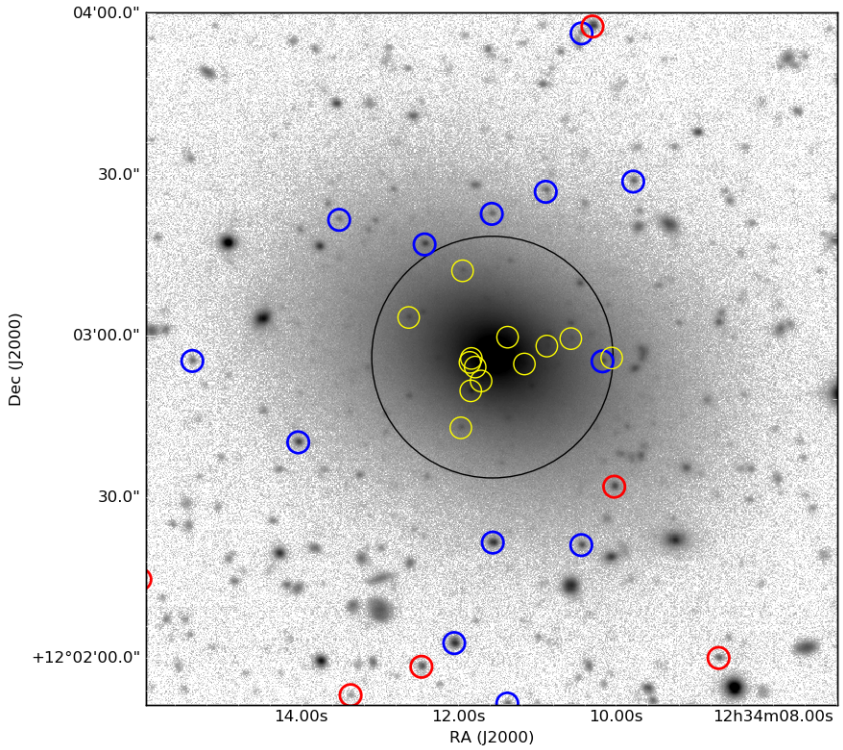

FIG. 2.— GC detection on VCC1545. The blue circles show the GCs detected both by our photometric method and HST data, yellow cirles show the GCs spectroscopically identified only, and red circles show the GCs detected only by our photometric criteria. The matching of the two methods is quite good outside central area (black circle, which indicates the half-flux radius, $r_e = 24.1$ arcsec), but is poor inside it, this is probably due to the special object extracting method of NGVS so that it cannot resolve objects too close to the galaxy center very efficiently.

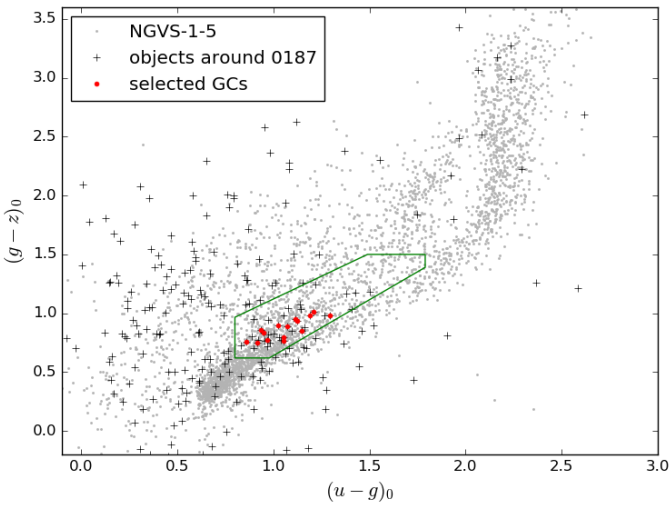

FIG. 3.— Color-color diagram selection of GCs. Gray dots are the objects in `NGVS-1-5` field brigher than $g = 22$, cross markers are the objects within R_c of 0187, and red dots are identified GCs. The area enclosed by the green polygon is GC selection criteria by color.

nitude) for early type galaxies(see fig.15 in Cote et al. (2006) and Brodie and Strader (2006));.

2.3. *Verification of nuclei*

We use GALFIT with King+Sérsic model to fit the dE,Ns, in order to verify that all the galaxies in our sample do have a nucleus. The determination of a nucleus is by the ratio of luminosty of nuleus and total luminosity of the galaxy $L_{\rm nuleus}/L_{\rm gal}$.[???]

All but one galaxy (0573) can be well fitted by King+Sersic model. 0573 cannot be fitted using King+Sérsic model, so we used double Sérsic model instead.

3. RESULTS

3.1. *S_N against M_V*

We calculated $S_{\rm N}$ value for 20 dE,Ns by methods discribed above (summarized in table.1) and plotted our data alongside Peng et al. (2008)'s (P08) data in fig.4 Our sample is deeper than P08, so we can explore the lower luminosity limit up to $\sim M_V = -13$.

We found that $S_{\rm N}$ of our dE,Ns are signifcantly higher than the typical value for mid-sized galaxies (whose $S_{\rm N}$ is usually on the order of unity), with only one $S_{\rm N}$ value under 5 and highest $S_{\rm N} = 62.7 \pm 4.2$(VCC0931). They also scatter more at low-luminosity end. Despite the scattering nature of $S_{\rm N}$ of dE,Ns, the average trend is clear, the larger M_V is (i.e. the fainter the galaxy is), the larger the $S_{\rm N}$, and it shows a sharp turn at about $M_V = -15.5$; this trend is summarized in table.2.

Among these 20 dE,Ns, we list below four galaxies that we think are kind of abnormal and probably need further investigation:

1. **0313,0573** These two galaxies have no distance module on NED, so we use 31.0. 0573(SDSS J123310.16+120509.9) has a very small $R_e = 2.56$ arcsec, and is not in VCC; no GC is found around it; it is not plotted.

TABLE 2
SPECIFIC FREQUENCY IN BINS OF M_V

M_V Range	$\langle M_V \rangle$	S_N
$(-24,-22)$[1]	-22.5	4.0
$(-24,-22)$	-22.5	5.4
$(-22,-21)$	-21.3	2.2
$(-21,-20)$	-20.5	1.3
$(-20,-19)$	-19.5	1.3
$(-19,-18)$	-18.7	1.7
$(-18,-17)$	-17.5	2.7
$(-17,-16)$	-16.5	3.3
$(-16,-15)$	-15.5	8.1
$(-15,-14)$	-14.5	24.4
$(-14,-13)$	-13.5	31.8

[1] Not including VCC 1316 (M87)
[2] These bins have combined data from this work and Peng et al. (2008)

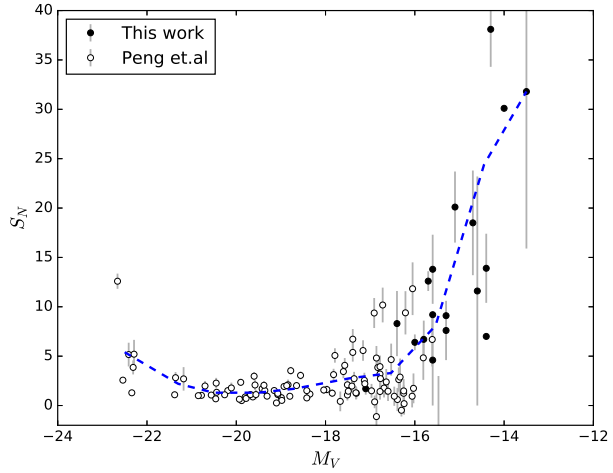

FIG. 4.— S_N versus galaxy M_V using data from this work and Peng et al. (2008). The trend is that at low luminosity, specific frequency is significantly higher and more scattered. The blue dash line shows the average trend of combined data. It is worth noticing that our data is much fainter.

2. **0042=IC3142** It has distance modulus=26.17 in NED, which is about 1.72Mpc, if so, it is definitely not a member of Virgo Cluster. Its DM is manually set to 31.0 (average for Virgo Cluster).

3. **0146=VCC0931** It has largest $S_{\rm N}$ and $S_{\rm N,z}$, generally not included in all discussion.

3.2. *S_N against M_z*

Following Peng et al. (2008), we also plotted $S_{N,z}$ against a redder band M_z in fig.5. The value of $S_{N,z}$ is obvoiously lower than V-band $S_{\rm N}$, because early galaxies are more luminous in z band than V band. The average trend (blue dashed line) looks similar to that in $S_{\rm N} \sim M_V$ relationship, as it also keeps low in mid-luminosity range and shows a sharp uprise at $M_z = -16.5$ toward the low luminosity end.

3.3. *environmental dependence*

We investigate the $S_{\rm N}$ dependence on environment by relating them to the projected distance

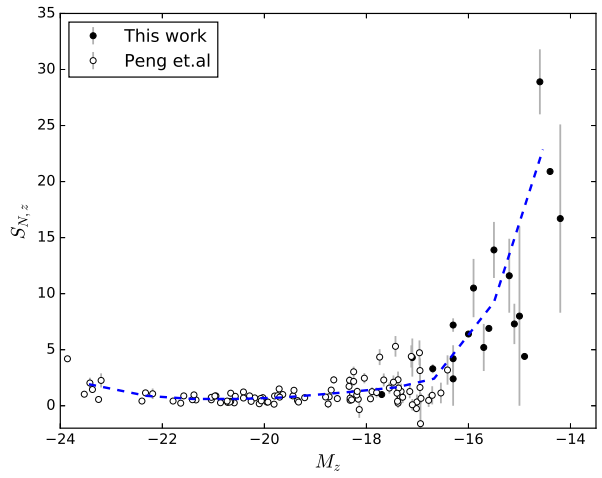

FIG. 5.— $S_{N,z}$ versus galaxy M_z. $S_{N,z}$ is clearly lower than $S_{\rm N}$, but scattered all the same. Blue dash line is the same as in fig.4

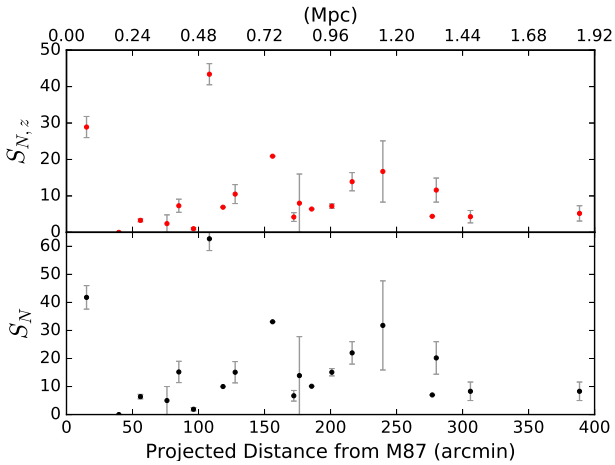

FIG. 6.— $S_{\rm N}$ and $S_{\rm N,z}$ against projected distance from M87

(r_p) from the dE,Ns to the galaxy cluster center, M87($12^{\rm h}30^{\rm m}49.4^{\rm s}, +12°23'28''$). In fig.6 we plotted both $S_{\rm N}$ and $S_{\rm N,z}$ against r_p and we see no significant trend for $S_{\rm N}$ environmental dependence from our result perhaps because of our small sample, although several researches pointed out that dEs near cluster center tend to have larger $S_{\rm N}$. The reason why $S_{\rm N}$ doesn't show environmental dependence in our sample is that: ...

3.4. *color distribution*

We detected 144 GCs in total around all 20 dE,Ns, the color distribution of them in $g-z$ is illustrated in fig.7. After fitting the histogram by a gaussian fit, we found the GCs are mainly blue with $g-z = 0.88$ and $\sigma = 0.10$; there is no significant bimodality and it seems that the dE,Ns in our sample don't pocess red GCs, which indicates that they have different GC formation history with giant galaxies whose GC systems usually show bimodality. Investigations on color distributions of individual dE,Ns cannot be made because each of them has so few GCs to show any significant trend in color individually.

4. DISCUSSION

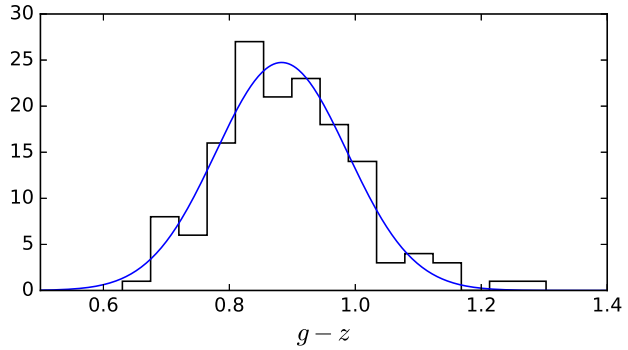

FIG. 7.— The color distribution histogram of all 144 GCs detected in $g-z$. The gaussian curve is fitted using `scipy.optimize.curve_fit`, peak at $g-z=0.88$, $\sigma=0.11$.

4.1. *Explanation for high S_N in dE,Ns*

There are generally two explanations for high S_N in dE,Ns. One is that these galaxies had a higher GC formation efficiency and thus intrinsically richer of GCs, and the other explanation is that field stars of dE,Ns are largely stripped (tidal striping? ram pressure stripping?) by surrounding massive galaxies but the GCs are still bound in the galaxies. Our work didn't find envronmental dependence, putting the discovery that dE,Ns in densed envrionment (cluster dwarfs) often have higher S_N and thus the latter explanation in question.

There are some models of GC formation efficiency and dE,N evolution history. The merger model,the dissipational accretion model and the stripping model.

4.2. *Problems and furture improvements*

What is the relation between S_N and T? Generally, T is considered a more physically intrinsic of GC richness to the galaxies, and is directly related to the GC formation efficiency history. But researchs still use S_N a lot because T is hard to get, as it needs complicated method converting observed flux to mass of galaxy. Also there is debate about which mass should T be normalized to, is it stellar mass $M_\star$ or dynamical mass M_{dyn} or other ways to measure mass? On the other hand, for luminosity scaled S_N , although there is suggestion that we should use z band or infrared wavelengths when normalizing, it is easier to get and can be a proxy indirectly but effectively related to GC formation efficiency.

we suffer from small scale of the sample. Our sample only include homogeneously 20 dE,Ns, so the results have inevitable uncertainties, so next we will do more dwarf galaxies from NGVS data and from other sources.

How good the counting is? We should improve on error estimation; the radius for counting GCs (R_c) and radius for counting contaminations are basically determined intuitively, so we hope to find a better way to set a standard fo choosing a convincing radius. There is another way to count GCs without specifying which object is GC and which one is not (see Zaritsky et al. (2015)). This method is based on the assumption that the GC spatial distribution around a galaxy follows a radial power law and other point sources does not, after fitting a power law to all the point sources (or not too diffused ones) detected, the non-GC sources can be substracted as a uniform background, then by integrating within a reasonable radius range, the researchers can get the total number of GCs around a galaxy.

Because of the faintness of the dE.Ns and lack of features, we are not able to distinguish them efficiently by auto-selection. Next we shall find out away to efficiently select them by computers.

5. CONCLUSION

We confrimed the U-shape in $S_N \sim M_V$ relationship at low luminosity end. Our result favors the stripping model (or intrinsically quenching model?).

1. U-shape. We explored the low-luminosity end of S_N and confirmed that S_N increase with absolute magnitude when luminosity is low.

2. environmental dependence. We found no sginificant envrionmental dependence

3. color distribution. Our dE,N sample only have blue GCs.

4. physical evolution history. No idea

This research made use of Astropy, a community-developed core Python package for Astronomy (Astropy Collaboration, 2013). This research has made use of the NASA/IPAC Extragalactic Database (NED) which is operated by the Jet Propulsion Laboratory, California Institute of Technology, under contract with the National Aeronautics and Space Administration. SDSS and NGVS

REFERENCES

W. E. Harris and S. van den Bergh, Astron. J. **86**, 1627 (1981).
E. W. Peng, M. Takamiya, M. J. West, L. Ferrarese, J. L. Tonry, and A. A. West, Astron. J. pp. 197–224 (2008).
S. Zepf and K. Ashman, Mon. Not. R. Astron. Soc. **264**, 611 (1993).
J. P. Brodie and J. Strader, Annu. Rev. Astrophys. pp. 193–267 (2006).
I. Y. Georgiev, T. H. Puzia, P. Goudfrooij, and M. Hilker, Mon. Not. R. Astron. Soc. **406**, 1967 (2010), arXiv:1004.2039v1.
W. E. Harris, G. L. H. Harris, and M. Alessi, Astrophys. J. **772**, 82 (2013), 1306.2247.
L. Ferrarese, P. Côté, J.-C. Cuillandre, S. D. J. Gwyn, E. W. Peng, L. A. MacArthur, P.-A. Duc, A. Boselli, S. Mei, T. Erben, et al., Astrophys. J. Suppl. Ser. **200**, 4 (2012), ISSN 0067-0049.
C. Liu, E. W. Peng, P. Côté, L. Ferrarese, A. Jordán, J. C. Mihos, H.-X. Zhang, R. P. Muñoz, T. H. Puzia, A. Lançon, et al., Astrophys. J. **812**, 34 (2015).
P. Cote, S. Piatek, L. Ferrarese, A. Jordan, D. Merritt, E. W. Peng, M. Haegan, J. P. Blakeslee, S. Mei, M. J. West, et al., Astrophys. J. Suppl. Ser. **165**, 57 (2006), 0603252.
D. Zaritsky, M. Aravena, E. Athanassoula, A. Bosma, S. Comerón, B. G. Elmegreen, S. Erroz-Ferrer, D. A. Gadotti, J. L. Hinz, L. C. Ho, et al., Astrophys. J. **799**, 159 (2015), arXiv:1411.4615v1.